Kääb, A. (2001): Photogrammetric reconstruction of glacier mass-balance using a kinematic ice-flow model. A 20-year time series on Grubengletscher, Swiss Alps. *Annals of Glaciology*. 31. 45-52.

Dr. Andreas Kääb
Department of Geography
Division of Physical Geography
University of Zurich - Irchel
Winterthurerstrasse 190
CH - 8057 Zurich
Switzerland

Phone: ++41 1 635 5146
Fax: ++41 1 635 6848
e-mail: kaeaeb@geo.unizh.ch

Photogrammetric Reconstruction of Glacier Mass-Balance using a Kinematic Ice-flow Model. A 20-year Time-Series on Grubengletscher, Swiss Alps.

ANDREAS KÄÄB

Department of Geography, University of Zurich, Winterthurerstr. 190, 8057 Zurich, CH

ABSTRACT. The kinematic boundary condition at the glacier surface can be used to provide glacier mass-balance at individual points if changes in surface elevation, horizontal and vertical surface velocities, and surface slope are known. Vertical ice velocity can in turn be estimated from basal slope, basal ice velocity and surface strain. This relation is applied to reconstruct a 20-year mass-balance curve of Grubengletscher (Swiss Alps) largely using repeated aerial photogrammetry but only a minimum of field work. For individual years the mass-balance distribution on the glacier tongue was modelled with an accuracy of about ±0.9 m a^{-1}. Ice-mechanical assumptions and errors in glacier-bed geometry markedly affect discrete mass-balance patterns but are eliminated to a major extent when calculating year-to-year mass-balance changes. The resulting curve for the Grubengletscher tongue 1973-1992 shows reasonable consistency with meteorological data and other glaciologically-derived mass-balance series. Large changes in measured ice speed on the glacier tongue (±50%) significantly governed the long-term variability of ice thickness over the observational period.

INTRODUCTION

Investigating glacier mass-balance is one of the main research activities in glaciology. Measuring mass-balance helps detecting climate variations, it contributes to the understanding and modelling of glacier reaction, and it assists hydrological applications and hazard assessment, to mention only some issues. Traditionally, glacier mass-balance is measured by scattered „representative“ in situ samples (mostly using stakes), an often time-consuming and expensive method, which gives, nevertheless, no area-wide mass-balance distribution but requires spatial interpolation. Additionally, conventional mass-balance measurements are difficult on debris-covered ice and in icefalls. These facts markedly render monitoring time-series of mass-balance more difficult. Therefore, longer mass-balance curves are only available for a limited number of glaciers (IAHS(ICSI)/UNEP/UNESCO, 1999). Several approaches of direct mass-balance determination have been tested to overcome these difficulties. Reynaud and others (1986), for instance, used transverse velocity profiles and measured elevation changes to calculate the mass-balance of longitudinal glacier sections. Rasmussen (1988) obtained both bed topography and mass-balance distribution iteratively, using repeated aerophotogrammetric measurements of elevation and displacements on Columbia Glacier, Alaska. An approach similar to one presented here is developed by Reeh and others (1999) in order to analyse and process surface velocity data obtained from satellite InSAR. In our contribution, we apply a remote sensing-based method, which was developed by Kääb (1996), and is also explained in detail by Kääb and Funk (1999) and Kääb and others (1998). Kääb and Funk (1999) used the kinematic boundary condition at the glacier surface to calculate the mass-balance distribution of a single year on Griesgletscher (Swiss Alps). Due to model-inherent sensitivities and photogrammetric restrictions, the model was only tested for the flat ablation area, but gave a promising accuracy of ±0.7 m a^{-1} for individual mass-balance values. (For a similar application cf. Gudmundsson and Bauder, 1999). In the study presented here, we (I) apply the method on the more complex ablation area of Grubengletscher (Swiss Alps), and (II) extend it to a 20-year time-series of annual mass-balances, each step with no field measurements necessary over the observational period. After a site description, we explain the two model steps of our approach and the methods used to obtain the input data, and end with discussing the results of the single steps.

SITE DESCRIPTION

The 1.4 km^2 large and approximately 3 km long Grubengletscher is located in the Saas valley (Valais, Swiss Alps). The highest point of the accumulation area is the Fletschhorn (3993 m a.s.l.). The partially debris-covered tongue reaching down to ca. 2770 m a.s.l. is situated nearby a conspicuous rock glacier, two cirque-glaciers formerly connected to the main glacier, and a number of periglacial lakes (Fig. 1; cf. Kääb and others, 1997). In 1968 and 1970 outburst floods from an ice-dammed lake and subsequent debris flows caused heavy damages in the nearby village Saas Balen (Röthlisberger, 1979). Since then, a number of investigations was started, mostly aiming at early recognition of lake outbursts, and preparing and assisting related protection works (Kääb, 1996; Kääb and others, 1997; Haeberli and others, 1999; Haeberli and others (in prep)). Many data and insights of special importance for our study resulted from these works. However, the most essential basics for our study is high-precision aerial photography of the glacier

tongue, which is almost annually taken in autumn by the Federal Office of Cadastral Surveys since 1970 (flying-height above ground: ca. 1000 m, image scale: ca. 1:7000; Kääb and others, 1997). Additionally, suitable photographs covering the entire glacier are available for perennial intervals from the Federal Office of Cadastral Surveys and the Federal Office of Topography.

MODEL AND ASSUMPTIONS

The model we use to reconstruct a mass-balance series of Grubengletscher follows two steps: (I) calculating the mass-balance distribution on the glacier tongue for single years using the kinematic boundary condition at the surface, and (II) deriving a mass-balance series from the single-year mass-balances.

Kinematic boundary condition at the surface

The kinematic boundary condition at the glacier surface can be used to provide glacier mass-balance at individual points as a function of changes in surface elevation, horizontal and vertical surface velocities, and slope. Vertical ice velocity can in turn be estimated from basal slope, basal ice velocity and surface strain. The relation is derived from mass conservation in a vertical column over the entire ice thickness (Hutter, 1983; Paterson, 1994; Kääb, 1996; Kääb and Funk, 1999). We use it in the form

$$b(x,y) = \frac{\partial z_s}{\partial t} + u_s \frac{\partial z_s}{\partial x} + v_s \frac{\partial z_s}{\partial y} - w_s \qquad (1)$$

with

$$w_s = u_b \frac{\partial z_b}{\partial x} + v_b \frac{\partial z_b}{\partial y} + \int_{z_b}^{z_s} \dot{\varepsilon}_{zz}\, dz \qquad (2)$$

where b is the mass-balance at a point (x,y) , z_s is the surface elevation, $\frac{\partial z_s}{\partial t}$ is the change in surface elevation with time, u_s and v_s , or u_b and v_b, respectively, are the horizontal velocity components at the surface or the glacier bed, $\frac{\partial z}{\partial x}$ and $\frac{\partial z}{\partial y}$ are the accordant slope components, w_s is the vertical surface velocity, z_b is the bed elevation, and $\dot{\varepsilon}_{zz}$ is the vertical strain-rate.

In our study, we try to determine all terms on the right hand side of Equations (1) and (2) and, subsequently, to calculate the mass-balance distribution on the glacier tongue point by point. Surface slopes, changes in surface elevation and horizontal surface velocities are derived from repeated photogrammetry. Bed topography and ice thickness is obtained from ground-based geophysical soundings. (See methods). The basal velocity (sliding and sediment deformation) is estimated by comparing measured surface velocities with a simple flow-law assumption (usual flow-law parameters, a shape factor of 0.8 and surface slope averaged over a distance of about ten times the ice thickness) and applying the simple relation

$$u_b \approx \beta \cdot u_s \qquad (3)$$

(analogous for v_b). We obtained a general ratio of basal velocity to total surface velocity

of about 90 % ($\beta \approx 0.9$) which varies less than ±5% due to temporal ice-thickness changes and uncertainties in the flow-law parameters. This estimation, of course, implies a large inaccuracy with potentially noticeable spatial and temporal variations.

Observed surface velocities of up to 45 m a^{-1} (see results), which are unexpectedly high in respect of the low slope on the glacier tongue, are the expression of this high basal velocity. The following facts might be possible causes for this high basal velocity: non-frozen sand and silts with a thickness of 100 m and more exist beneath the glacier tongue and could allow for high sediment deformation rates (Haeberli and Fisch, 1984; cf. Haeberli, 1981). Observations in an ice tunnel near the ice-dammed lake (Haeberli, 1976; cf. Röthlisberger, 1979) and on the glacier surface (see mass-balance distribution) provide indications of intraglacial shearing. From field work in the 1970's the tongue is known to have been partially frozen to its bed at the margins (Haeberli, 1976). This marginal sealing led to high subglacial water pressure, expressing itself in artesian water sourcing from boreholes. The latter couldn't be observed on a second drilling campaign in the mid 1990's. Finally, the several hundred metres long tongue itself is flat (less than 10°), while the adjacent glacier parts are much steeper (25-30°) a precondition which might cause some pushing of the entire ice column additional to deformational stress coupling.

The second estimation which is needed to solve the kinematic boundary condition is the variation of strain-rate with depth (cf. Equation (2)). Again, we use a very rough approach assuming a linear relation between the total vertical strain at the surface ε_{zz_s}, and the ice thickness h and the vertical surface strain-rate $\dot{\varepsilon}_{zz_s}$ on the other hand:

$$\varepsilon_{zz_s} = \int_{z_b}^{z_s} \dot{\varepsilon}_{zz}\, dz \approx \gamma \cdot h \cdot \dot{\varepsilon}_{zz_s} \quad . \qquad (4)$$

The horizontal surface strain-rates were derived from the velocity fields using a method proposed by Nye (1959), and the vertical surface strain-rates were obtained from the incompressibility condition $\dot{\varepsilon}_{xx} + \dot{\varepsilon}_{yy} + \dot{\varepsilon}_{zz} = 0$. Considering the high ratio of basal velocity, a γ of 1.0 was introduced (cf. Kääb and Funk, 1999; Gudmundsson and Bauder, 1999). As for the estimate of the basal velocity, we presume a potentially large spatial and temporal uncertainty of the latter assumption.

Using the above two ice-mechanical estimations, and photogrammetric and geophysical measurements it is possible to finally compute the mass-balance distribution on the glacier tongue for a single year, which represents the first step of our model-chain towards reconstructing a mass-balance curve. One remaining problem, however, consists in potential errors in the glacier bed determination, especially if the geophysically-derived bed topography (for instance the ice-sediment transition) does not coincide with the 'kinematic' bed, i.e. the basal horizon used in the kinematic boundary condition. (Cf. mass-balance distribution).

Mass-balance variations

From Equations (1)-(4) it can be seen that the effect of measurement errors and faulty ice-mechanical assumptions will increase with increasing basal velocity, increasing bed and surface slope, and increasing ice thickness and strain-rates. Thus, single mass-balance

values calculated for Grubengletscher will potentially have a much larger error than, for instance, for the planar and slow flowing tongue of Griesgletscher (Kääb and Funk, 1999). Independently of the valuable conclusions about ice-flow characteristics which can be drawn from such analyses (see results), we are here interested in mass-balance variations with time more than in the absolute accuracy of individual mass-balance values or in the distribution pattern. In this second step of our model-chain, the effects of the uncertainties of our estimations and of measurement errors are reduced in two ways: (a) The reconstruction of the mass-balance series for the glacier tongue requires only one average mass-balance value per year for the tongue. Spatial averaging of each annual mass-balance distribution to one average value will eliminate the error components of high spatial frequency and random noise to some extent. Absolute deviations will, nevertheless, remain. (b) The mass-balance variation Δb for individual points is basically derived from differences of the Equation-set (1)-(4) between two years:

$$\Delta b = \Delta\left(\frac{\partial z_s}{\partial t}\right) + \Delta\left(u_s \frac{\partial z_s}{\partial x}\right) + \Delta\left(v_s \frac{\partial z_s}{\partial y}\right) - \Delta\left(\beta u_s \frac{\partial z_b}{\partial x}\right) - \Delta\left(\beta v_s \frac{\partial z_b}{\partial y}\right) - \Delta\left(\gamma\, h\, \dot{\varepsilon}_{zz_s}\right) \quad (5)$$

In Equation (5) the first three terms, and the surface velocity and vertical surface strain-rate in the fourth, fifth and last term, can be directly derived from photogrammetric measurements. A time-constant component of the error in β would be eliminated if one assumed both surface velocity and bed slope being constant with time (analogously for an error in bed slope); a time-constant component of the error in γ would be eliminated if one assumed both strain-rates and ice thickness constant with time (analogously for an error in ice thickness). The assumption of constant bed slope will certainly apply to a major extent on a year-to-year time scale. Surface velocities, strain rates and ice thickness varied by not more than 10% from one year to the following over the observational period. Thus, only errors of second order will remain when calculating annual mass-balance variations and fixing the whole series to its temporal average.

METHODS

Solving the kinematic boundary condition Equations (1)-(4) requires the annual surface topography and the annual surface velocity field of the Grubengletscher tongue, as well as the glacier bed topography. In our study, primarily aerophotogrammetric techniques are used to obtain the above data. Surface slopes and changes in surface elevation (cf. Equation (1)) are derived from totally 21 DEMs, each with 25 m regular grid-spacing and including about 1000 points. Gaps in this time-series (cf. Fig. 11 top) are due to missing photography. The height values of the DEMs have an accuracy of about ±0.2 m a^{-1} (RMS) and the elevation changes one of about ±0.3 m a^{-1}.

For seven individual years, irregularly distributed over the observational period, aerial photography of the entire glacier (image scales from 1:11 000 to 1:20 000) was available to determine complete DEMs of the glacier and related elevation changes (50 m resolution and about 700 points each DEM). In this contribution, only data of the glacier tongue are used. However, the elevation changes of the entire glacier are also displayed for comparison (cf. Fig. 1 and 2).

While the DEMs were derived from repeated monotemporal photogrammetric stereo-pairs, the surface velocities were determined by a special procedure simultaneously

comparing two aerial photographs taken at different times and from different positions (so-called multitemporal stereo-models). The spatial resolution of the obtained velocity fields is similar to the one of the DEMs. Due to photogrammetric restrictions (e.g. insufficient optical contrast) and missing photography, a reduced number of 14 velocity fields has been measured. The accuracy of a individual displacement-vector, deduced by comparison with stake measurements, is about ±7 % , that is ±1.7 m a^{-1} in average for the Grubengletscher tongue. Various photogrammetrically-derived data of Grubengletscher have been determined from 1967 to 1995, whereas a complete overlapping data-set with DEMs and velocity data as needed for our model is only available for the period 1973-1992. Details on the used photogrammetric techniques, related accuracy and post-processing procedures are described in Kääb (1996), Kääb and others (1997), and Kääb and Funk (1999). The propagation of photogrammetric errors towards the calculations of vertical ice velocity and mass balance (Equations (1) and (2)) is evaluated in Kääb and Funk (1999).

The bed slope and the ice thickness (cf. Equations (2) and (4)) were derived from the glacier bed topography. Haeberli and Fisch (1984) compiled it from radio-echo soundings and hot water drilling with borehole electrodes, obtaining also valuable information about the subglacial sediment layer (see model and assumptions). In the most places the accuracy of the measured ice thickness is about 5% with possible single errors of about 10% or more. Post-processing procedures for the ice-thickness data are described in Kääb (1996) and Kääb and Funk (1999).

RESULTS

Surface kinematics

In the following section we describe and discuss the input data as well as the results of our calculations. Figure 2 depicts the cumulative changes in elevation of the Gruben glacier as derived from DEMs of the entire glacier and the tongue. The spatial distribution of the elevation changes is exemplified for the periods 1975-1985-1991 (Fig. 1). During 1967-1995 Grubengletscher experienced three different major periods of volume change: from 1967 to 1975 (1976 for the tongue) the average elevation remained nearly constant and the tongue thinned by about -0.2 m a^{-1}. During the period from 1975 (1976) to 1985 the glacier became thicker by about +0.25 m a^{-1} (+0.5 m a^{-1} for the tongue), a development which is known as '1980's maximum' for many other Swiss glaciers and could, in a similar form, also be observed for the nearby Gruben rock glacier (Kääb and others, 1997). From 1985 to 1991 (1995) the glacier thinned considerably by -0.8 m a^{-1} (-0.6 m a^{-1} for the tongue). The elevation changes on the glacier tongue are attenuated by the heavy debris-coverage of the lowest part (cf. Fig. 3). Average annual changes on the debris-free part range from +1.5 m a^{-1} to –2 m a^{-1} for the above periods (approximately ±5 % of ice thickness per year). The only surface rise during 1985-1991 happened to the north-west (NW) of the tongue where a distinct advance of totally about 50 m (horizontal distance) during 1975-1985 did continue over the last period to a reduced extent. Surprisingly at a first view, the advance did not take place at the terminus close to the moraine lake but rather laterally. The advance clearly followed the today's main flow direction (Fig. 4; cf. Kääb and others, 1997).

In the following presentation of results the mass-balance year 1979/80 will serve as

an example for our spatial calculations. Figure 3 shows the changes in surface elevation $\frac{\partial z_s}{\partial t}$ over that period. In 1979/80 the glacier tongue experienced the largest increase of ice thickness over the observational period (cf. Fig. 11 top). The raw measurements (25m spacing) were smoothed (cf. Kääb and Funk, 1999) and are depicted with 50m spacing. Even so, a smooth pattern for the debris-free ice and more erratic spatial variations with generally lower elevation changes for the debris-covered ice can be distinguished.

Figure 4 gives three examples of the 14 determined horizontal velocity fields. Due to photogrammetric and terrain restrictions measurements were not possible for the complete tongue. The partially scattered data were interpolated to a 50 m-grid. As can be seen from Figure 11 (top) showing the horizontal surface speed averaged for the entire tongue, the velocity fields given in Figure 4 represent approximately minimum and maximum stages during the observational period. Maximum speeds observed at individual points amount up to 30 m a^{-1} between 1973 and 1974 (1973/74), up to 45 m a^{-1} in the year 1979/80, and about 25 m a^{-1} in the year 1991/92. The drastic changes in surface speed (almost 50 % in ten years; Fig. 11 top) coincide only very roughly with the development of ice thickness (Fig. 2). The ice speed decreased from the beginning 1980's, whereas the surface elevation did later from the mid 1980's, both together indicating that the variations of speed were not governed by the variations of ice thickness during the 1970's and 1980's. The latter observation and the estimated high basal velocity (cf. model and assumptions) suggest that some subglacial effect (water pressure?) may mainly be responsible for the velocity changes. The velocity fields show a rather inactive terminus to the SW receiving only a minor part of the ice supply which is rather directed to the NW. Especially from 1973 to 1980, the SW- and the NE-part of the tongue experienced a different temporal behaviour suggesting that the tongue may be dynamically divided, which might also be underlined by the different debris coverage of the SW- and NE part of the ablation area. Between 1979 and 1992, generally representing a phase of glacier thinning, a small clockwise rotation of flow direction occurred in the NW part of the tongue .

The horizontal and vertical surface-strain rates were calculated from the horizontal velocity fields. Both are exemplified for 1979/80 including the crevasse-pattern mapped for 1980 (Fig. 5 and 6). Strong longitudinal compression of over 0.1 a^{-1} can be found in the SW-part compared to markedly smaller values to the NE. A zone of horizontal extension coincides with the observed crevasses with respect to their location and direction. Compressive flow clearly prevails on the Grubengletscher tongue, as generally expected for ablation areas. Some features of extensive flow can be attributed to the topographically-induced widening of the flow field.

Details on the glacier bed topography (Fig. 7), our last missing model input, can be obtained from Haeberli and Fisch (1984). It should, however, pointed out that the direction of the bed-trough rotates from NW-direction in the upper part to SW-direction in the lower part, which cannot be observed to such a distinct extent in the flow field (Fig. 4). Thus, an upward flow-component towards the ice-dammed lake is the result.

Mass-balance distribution

The distribution patterns of the vertical ice velocity at surface and the mass-balance calculated from Equations (1)-(4) are illustrated for the year 1979/80 (Fig. 8 and 9). The general pattern of the calculated vertical ice velocity at the surface w_s (Fig. 8) with

negative values in the upper part and positive values in the lower one seems to reflect mainly the bed slope with respect to the flow direction (cf. above discussion of bed topography). The small negative or even positive values in the SE-part are caused by a little plain or bump in the bed data. Model-tests showed that the results of w_s are quite sensitive to a smoothing of the bed data affecting particularly this bump.

The final mass-balance distribution (Fig. 9) is questionable in some parts. While negative values predominate as expected, some positive values are hard to explain. They have to be attributed to errors in our ice-mechanical assumptions or faulty bed topography more likely than to errors in the photogrammetric data. The small positive and negative values for the heavily debris-covered ice to the SW make sense in the way that a erratic mass-balance distribution highly dependent on the local characteristics of the morainic cover could be expected there. However, the micro-topography of this area (large boulders of 2-5 m diameter) markedly complicate the photogrammetric measurements and the model applicability. Surface slopes and elevation changes, derived from 25m-spaced measurement points, could partially be affected by individual boulders not sufficiently representing their surrounding topography. These problems are illustrated by the changes in elevation for 1979/80 (Fig. 3) which show irregular spatial variations for the debris-covered ice. A general dependence of mass-balance on elevation can neither be seen from the distribution pattern for 1979/80 nor for other years. However, this seems not astonishing in view of the small elevation range of the investigated glacier part and, on the other hand, the large spatial variations of debris coverage and relief parameters (slope, aspect, roughness etc.) influencing differential ice melt.

For the year 1979/80 the results can be compared with some geodetic and glaciological stake measurements (Fig. 10). Whilst similar investigations on Griesgletscher – carried out under more favourable conditions with respect to model applicability – gave an accuracy of ±0.3 m a^{-1} for the vertical ice velocity at surface and of ±0.7 m a^{-1} for the mass-balance (Kääb and Funk, 1999), the results presented here are heavily affected by the assumptions and model-sensitivities. Errors in bed slope, β, γ or ice thickness, for instance, have a large influence on the calculated vertical ice velocity due to the high basal velocity, large strain-rates and complex bed geometry (cf. Equations (2)-(4)). Ignoring stakes 22 and 24, the stake measurements and the calculations of the vertical ice velocity at surface agree within ±0.6 m a^{-1} in average. Assigned only to errors in the model parameters β and γ, this deviation would in average be equivalent to an error in β of ±0.2 or an error in γ of ±0.5, respectively. Thus, for the Grubengletscher conditions our model is more sensitive to the estimation of the basal velocity Equation (3) than to the one of the vertical strain rate variation Equation (4).

We attribute the large deviation for stake 22 to an error in bed topography, which can consist in a difference between the geophysically-derived bed and the 'kinematic' bed and has not necessarily to be an error of geophysical bed determination. This first difference might play a part in case of stakes 11 and 24 where the actual vertical ice velocity (from stake measurements) reveals significant higher values than the calculated one. Sharp transverse vertical shear-horizons accompanied by 'fresh' sand and silts at the ice surface, and apparent longitudinal variations of debris geology in this zone confirm our hypothesis of a kinematic basal layer with steeper increase than derived from the geophysical soundings (cf. model and assumptions). The glacier might have overthrusted its frozen margins. The calculated mass-balance agrees with the measured one within

±0.9 m a^{-1} , ignoring again stakes 22 and 24. For these two positions the error in mass-balance can clearly be attributed to the error in calculated vertical ice velocity. The differences between calculated and measured values for w_s and b can be reduced by some adaptation of β and γ which can be seen from the fact that the linear regressions of the data points (without stakes 22 and 24; Figure 10) approximate slightly different lines than the depicted diagonal. With respect to these regressions the measured and calculated values agree in average within ±0.5 m a^{-1} for w_s (R^2 = 0.77) and within ±0.3 m a^{-1} for b (R^2 = 0.91).

Mass-balance variation

In our second model step we calculated the mass-balance variations 1973-1992 for the tongue from Equation (5). To obtain a continuous series, the mass-balance for years without available horizontal velocity data was modelled by introducing interpolated velocities in the kinematic boundary condition. This practice seems reasonable to us in respect of the smooth changes in surface velocity (cf. Fig. 11 top). The mass-balance for years with neither velocity nor elevation data was linearly interpolated, indeed an uncertain procedure but confirmed by comparison with measured mass-balance series in the Alps (cf. IAHS(ICSI)/UNEP/UNESCO, 1999). Figure 11 (middle) depicts the calculated time series shifted by +2.5 m a^{-1} to a zero-mean. For comparison purposes the mass-balance curve for the Griesgletscher tongue (2400-2700 m a.s.l.) as derived from stake measurements is included, shifted by +2.1 m a^{-1} to a zero-mean (Funk and others, 1997; IAHS(ICSI)/UNEP/UNESCO, 1999). Griesgletscher, about 40 km away from the Gruben area, is situated in the Swiss Central Alps and assumed to have roughly comparable climate conditions to Grubengletscher. Figure 11 (top) shows the photogrammetrically-derived annual changes in elevation and the average horizontal surface speed for the tongue, both governing the temporal variability of the calculated mass-balance (cf. Equation (1)). Furthermore, mean annual precipitation records and summer temperatures (July-October) are given for the station Grächen (1600 m a.s.l, about 10 km away from Gruben; Fig. 11 bottom; SMA, 1995). Comparing the curves of surface speed, elevation changes and calculated mass-balance clearly shows that the high frequencies of the elevation change are mainly controlled by the annual mass-balance, whereas the horizontal ice-velocities influence the lower frequencies. The climate records of Grächen, especially the observed variations in mean summer temperature, seem to confirm the mass-balance variations calculated for Grubengletscher tongue by a reasonable consistency. Furthermore, from 1973/74 to 1986/87 the calculated mass-balance curve for the Grubengletscher tongue and the measured one of Griesgletscher tongue show a quite good agreement. However, since 1987 this agreement between the two mass-balance curves is strongly reduced with no clear explanation available. Possible reasons could be a climatic difference between the two locations after 1987 or changing local glaciological conditions. The period of worse agreement after 1987 is a period of exceptional mass losses for most alpine glaciers, not only for Gruben- and Griesgletscher. Furthermore, it should be emphasized that the Griesgletscher tongue is entirely debris-free in contrast to the significant debris-coverage of the Grubengletscher tongue. Therefore, a different reaction of both glaciers to periods of strongly negative mass-balance could be expected to some extent considering, for instance, albedo changes of the white ice. It can be summarised that the calculated series of annual-mass balances for the Grubengletscher tongue appears reasonable in a great measure, whereas some

uncertainties still remain concerning the period after 1987.

PERSPECTIVES

The kinematic boundary condition at the glacier surface together with photogrammetrically-derived elevation and velocity data was shown to provide a valuable tool to model and analyse the spatial distribution and temporal variations of ice-flow and mass-balance. However, the usefulness of the presented test study on Grubengletscher is restricted by some particular characteristics, for instance with respect to debris coverage, bed geometry or ice dynamics. Due to photogrammetric restrictions for snow and firn areas the presented approach is, in the present stage, primarily suitable for ablation areas (cf. Kääb and Funk, 1999). The noticeable effects of the ice-mechanical assumptions and possible errors in the basal glacier horizon are eliminated to a major extent by modelling mass-balance variations from repeated photogrammetric measurements. On the one hand, such work requires extensive photogrammetric data acquisition, but on the other hand opens up a promising opportunity to remotely obtain detailed information on ice-flow and mass-balance, even for debris-covered ice or difficult-to-reach areas as icefalls. If not available by airborne radar-techniques, the only necessary field work, which is the determination of the glacier bed geometry, can be made up at any later time.

At the present stage, our approach seems especially promising for analysing ice-flow and mass-balance distribution of specific glaciers towards better process understanding. Related long-term mass-balance monitoring requires photogrammetric series with the same temporal resolution as the desired mass-balance, which will not be available for a large global number of glaciers in the near future. However, new remote sensing technologies in the field of digital photogrammetry, airborne optical and laser-scanning, air- and spaceborne synthetic aperture radar, and satellite imagery analysis will markedly raise the data availability and facilitate the data acquisition in glaciology. In view of this trend the presented approach might once be a suitable tool for remote sensing-based global glacier monitoring.

ACKNOWLEDGEMENTS

The presented study is mainly based on data which were collected at the Laboratory of Hydrology, Hydraulics and Glaciology (VAW, ETH Zurich), financially supported by the Swiss National Research Programme No. 31 on 'Climate Change and Natural Disasters'. We gratefully acknowledge the careful and constructive reviews of two anonymous referees. Sincere thanks are given to all colleagues providing useful discussions on the study and helping with field work, especially to W. Haeberli and R. Frauenfelder for their fruitful comments on the present contribution. The photogrammetric investigations would not have been possible without the valuable aerial photographs taken by the Federal Office of Cadastral Surveys. The geodetic works for establishing photogrammetric ground control points and the stake measurements were greatly assisted by W. Schmid and H. Bösch.

REFERENCES

Funk, M., R. Morelli and W. Stahel. 1997. Mass balance of Griesgletscher 1961-1994: different methods of determination. *Z. Gletscherkd. Glazialgeol* , **33**(1), 41-56.

Gudmundsson, G.H. and A. Bauder. 1999. Towards an indirect determination of the mass-balance distribution of glaciers using the kinematic boundary condition. *Geogr. Ann.,* **81A**(4), In press.

Haeberli, W. 1976. Eistemperaturen in den Alpen. *Z. Gletscherkd. Glazialgeol.* , **11**(2), 1975, 203-220.

Haeberli, W. 1981. Correspondence. Ice motion on deformable sediments. *J. Glaciol.,* **27**(96), 356-36**.**

Haeberli, W. and W. Fisch. 1984. Electrical resistivity soundings of glacier beds. A test study on Grubengletscher, Wallis, Swiss Alps. *J. Glaciol.,* **30**(106), 373-376**.**

Haeberli, W., A. Kääb, M. Hoelzle, H. Bösch, M. Funk, D. Vonder Mühll and F. Keller. 1999. Eisschwund und Naturkatastrophen im Hochgebirge. *Schlussbericht NFP31*. Zürich. vdf Hochschulverlag an der ETH Zürich. 190pp.

Haeberli, W., A. Kääb, D. Vonder Mühll and Ph. Teysseire. (in prep). Prevention of debris flows from outbursts of periglacial lakes at Gruben, Valais, Swiss Alps. submitted to J. Glaciol.

Hutter, K. 1983. *Theoretical glaciology; material science of ice and the mechanics of glaciers and ice sheets*. Dordrecht, etc., D. Reidel Publishing Co.; Tokyo, Terra Scientific Publishing Co.

IAHS(ICSI)/UNEP/UNESCO. 1999. *Glacier Mass Balance Bulletin No. 5, 1996-1997*. Haeberli W., M. Hoelzle and R. Frauenfelder, *eds*. World Glacier Monitoring Service, University and ETH Zürich.

Kääb, A. 1996. Photogrammetrische Analyse zur Früherkennung gletscher- und permafrostbedingter Naturgefahren im Hochgebirge. *Eidg. Tech. Hochschule, Zürich. Versuchsanst. Wasserbau, Hydrol. Glaziol. Mitt.* **145**, 182pp.

Kääb, A. and M. Funk. 1999. Modelling mass balance using photogrammetric and geophysical data. A pilot study at Gries glacier, Swiss Alps. *J. Glaciol.,* In press.

Kääb, A., G.H. Gudmundsson and M. Hoelzle. 1998. Surface deformation of creeping mountain permafrost. Photogrammetric investigations on rock glacier Murtèl, Swiss Alps. *In* Lewkowicz, A.G. and M. Allard, *eds*. *Proceedings of the 7th International Conference on Permafrost, Yellowknife, Canada.* Collection Nordicana. University Laval. 531-537.

Kääb, A., W. Haeberli and G.H. Gudmundsson. 1997. Analysing the creep of mountain permafrost using high precision aerial photogrammetry: 25 years of monitoring Gruben rock glacier, Swiss Alps. *Permafrost and Periglacial Processes,* **8**(4), 409-426.

Nye, J.F. 1959. A method of determining the strain-rate tensor at the surface of a glacier. *J. Glaciol.,* **3**(25), 409-419.

Paterson, W.S.B. 1994. *The physics of glaciers. Third edition.* Oxford, etc., Elsevier.

Rasmussen, L.A. 1988. Bed topography and mass-balance distribution of Columbia Glacier, Alaska, U.S.A., determined from sequential aerial photography. *J. Glaciol.,* **34**(117), 208-216.

Reeh, N., S.N. Madsen and J.J. Mohr. 1999. Combining SAR interferometry and the equation of continuity to estimate the three-dimensional glacier surface velocity vector. *J. Glaciol.,* In press

Reynaud, L., M. Vallon and A. Letreguilly. 1986. Mass-balance measurements: problems and two new methods of determinig variations. *J. Glaciol.,* **32**(112), 446-454.

Röthlisberger, H. 1979. Glaziologische Arbeiten im Zusammenhang mit den Seeausbrüchen am Grubengletscher, Gemeinde Saas Balen (Wallis). *Eidg. Tech. Hochschule, Zürich. Versuchsanst. Wasserbau, Hydrol. Glaziol. Mitt.* **41**, 233-256.

SMA. 1995. Annalen der Schweizerischen Metereologischen Anstalt. Zürich. **132**.

FIGURES

Fig. 1 Spatial pattern of elevation changes on Grubengletscher (Swiss Alps) for the periods 1975-1985 and 1985-1991. The strong increase of elevation to the north-west of the tongue indicates a glacier advance by about 50m. Contour lines in metres a.s.l. North-direction to the left.

Fig. 2 Cumulative changes in surface elevation of Grubengletscher and it's tongue for the period 1967-1995 as derived from repeated aerial photogrammetry . For the glacier tongue a much denser time-series of photography and related digital elevation models (indicated as dots) are available.

Fig.3: Annual changes in surface elevation ($\partial z_s / \partial t$) of the glacier tongue for the year 1979/80. The dashed line indicates the boundary of debris cover. North-direction upwards.

Fig. 4 Annual horizontal velocity fields of the glacier tongue for the years 1973/74, 1979/80 and 1991/92 indicating drastic changes in flow regime (cf. Fig. 11 top). The velocities quoted in the legend represent approximate maximum observed values for each period.

Fig. 5 Horizontal principal surface strain-rates during 1979/80 derived from the velocity field. The crevasses of 1980 were mapped photogrammetrically. The dashed line on the tongue indicates the boundary of debris cover (cf. Fig. 3). The straight and dashed parts of the glacier outline represent certain or uncertain, respectively, identification on the aerial photography.

Fig. 6 Vertical surface strain-rates ($\dot{\varepsilon}_{zz\,s}$) during 1979/80 calculated from the horizontal strain-rates assuming incompressible ice.

Fig. 7 Contour lines of glacier bed geometry (dashed lines, in m a.s.l) as determined by radio-echo soundings (after Haeberli and Fisch, 1974). Ice thickness of the central parts ranges from 20 m to 60 m in 1995, and up to 15 m more in 1985.

Fig. 8 Calculated vertical ice velocity (w_s) for 1979/80 including positions of stakes. The dashed line on the tongue indicates the boundary of debris cover (cf. Fig. 3). The straight and dashed parts of the glacier outline represent certain or uncertain, respectively, identification on the aerial photography.

Fig. 9 Calculated mass-balance pattern (b) for 1979/80 including positions of stakes.

Fig. 10 Comparisons between stake measurements of the vertical ice velocity (w_s) and mass-balance (b), and calculated values both for 1979/80. Mass-balance is not available for all stakes. The dashed lines represent linear regressions without the stakes 22 and 24 (see text).

Fig. 11 Average horizontal surface speed and elevation changes of the Grubengletscher tongue(top). Annual mass-balance variations calculated for the Grubengletscher tongue and measured for the Griesgletscher tongue (middle; the latter after Funk and others, 1997). Records of mean annual precipitation and mean summer temperatures (July-October) for the meteorological station Grächen (bottom). Note the rotated algebraic sign on the vertical axis for the temperature record. Bold dots in the graph of horizontal velocities indicate photogrammetric measurements of high accuracy (annual intervals, redundant measurements), whereas un-filled dots mark normal accuracy (partially perennial intervals). Analogously, un-filled dots in the mass-balance graph indicate calculations from the latter data (perennial intervals interpolated).

Kääb, A. (2001): Photogrammetric reconstruction of glacier mass-balance using a kinematic ice-flow model. A 20-year time series on Grubengletscher, Swiss Alps. *Annals of Glaciology*. 31. 45-52.

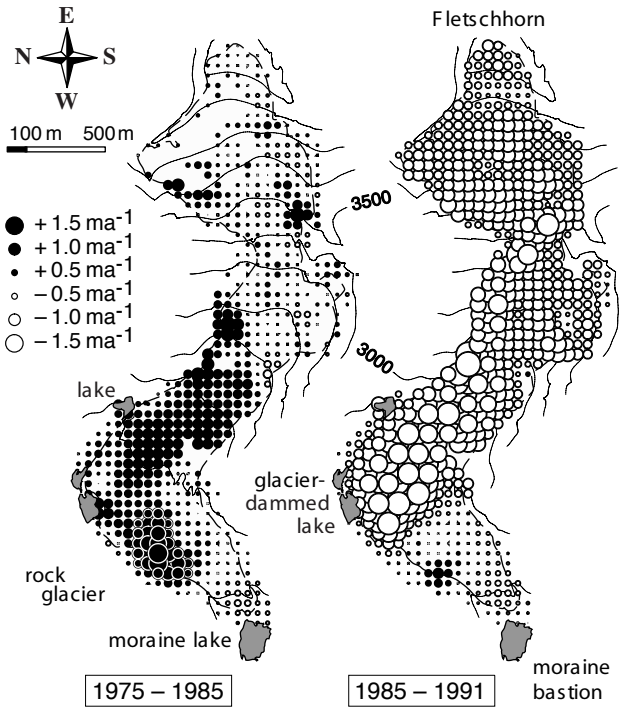

Figure 1

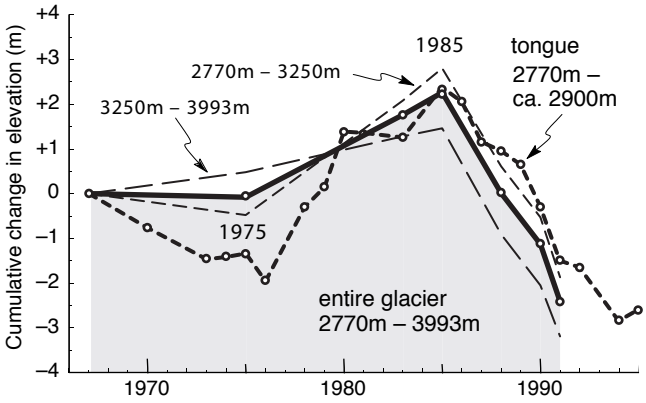

Figure 2

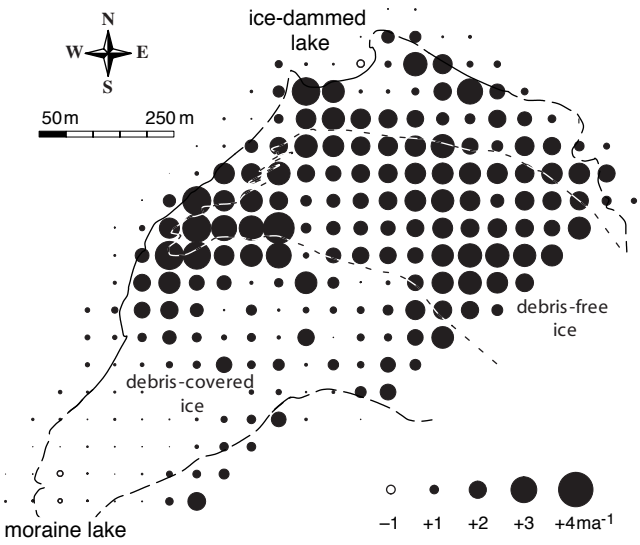

Figure 3

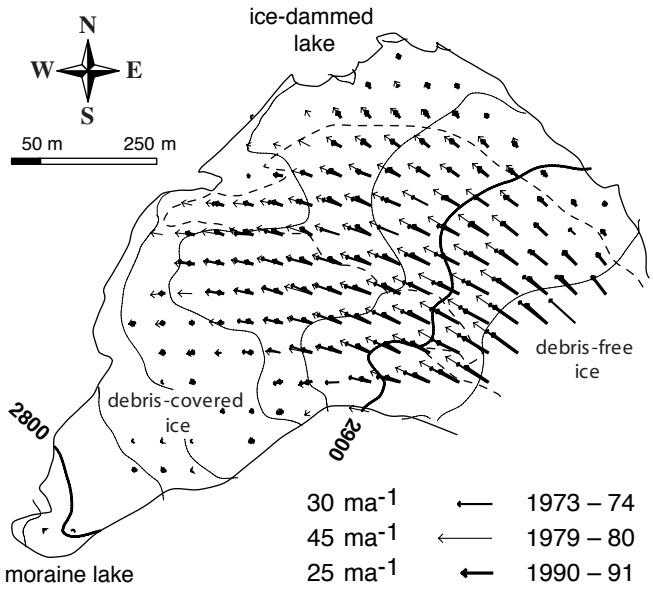

Figure 4

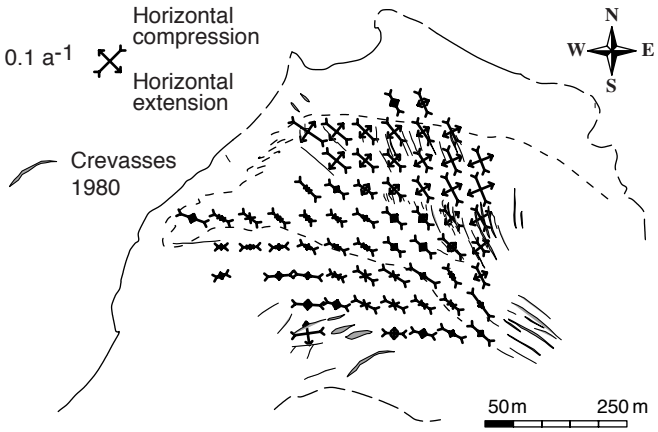

Figure 5

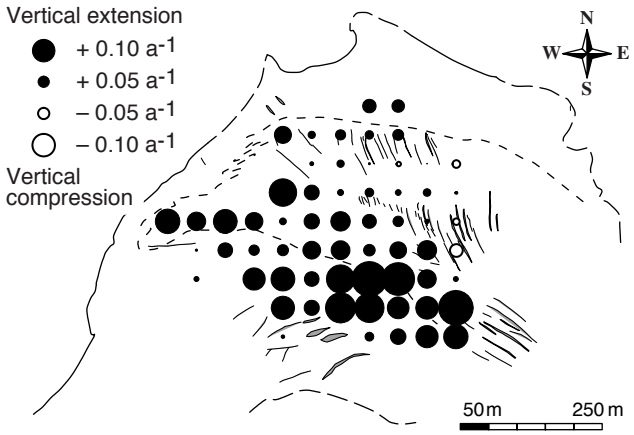

Figure 6

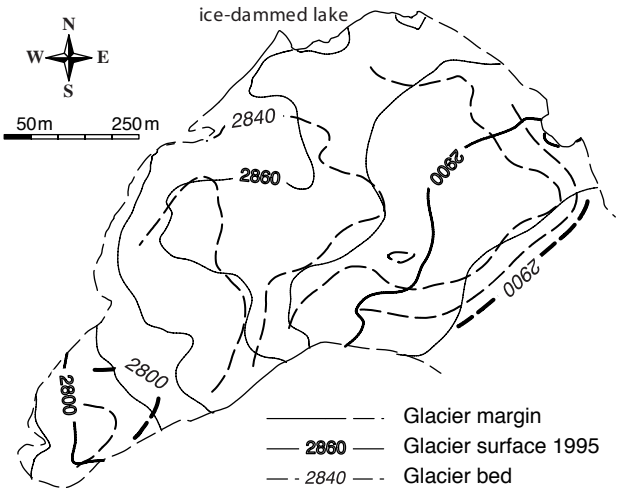

Figure 7

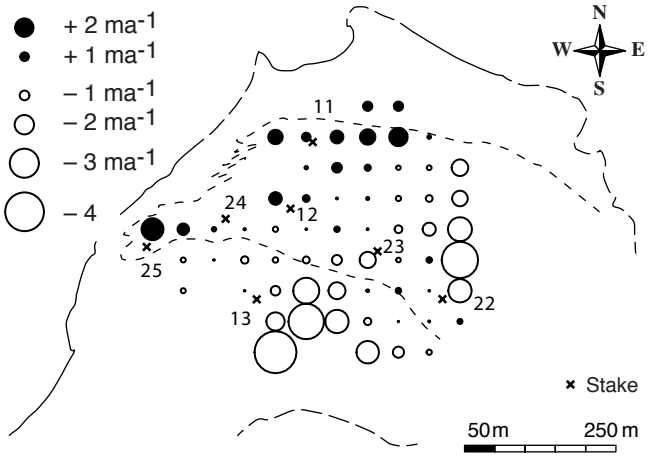

Figure 8

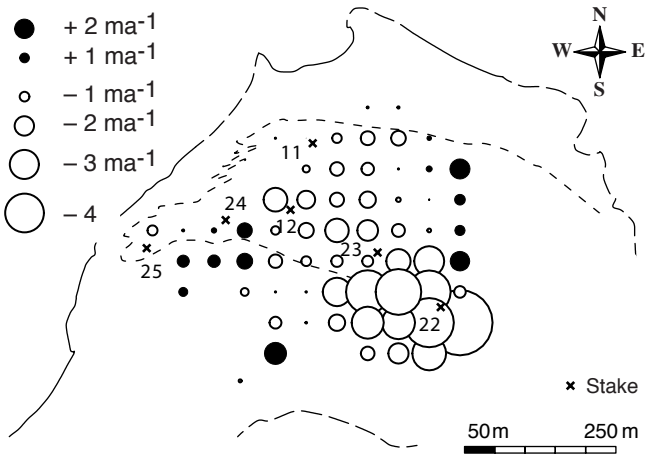

Figure 9

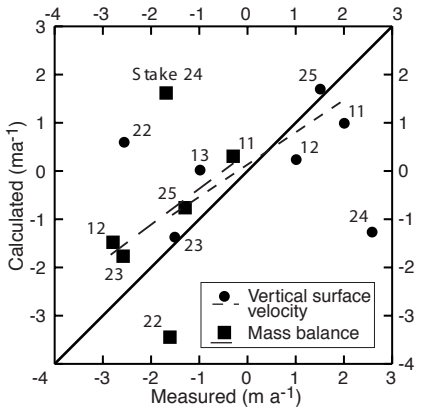

Figure 10

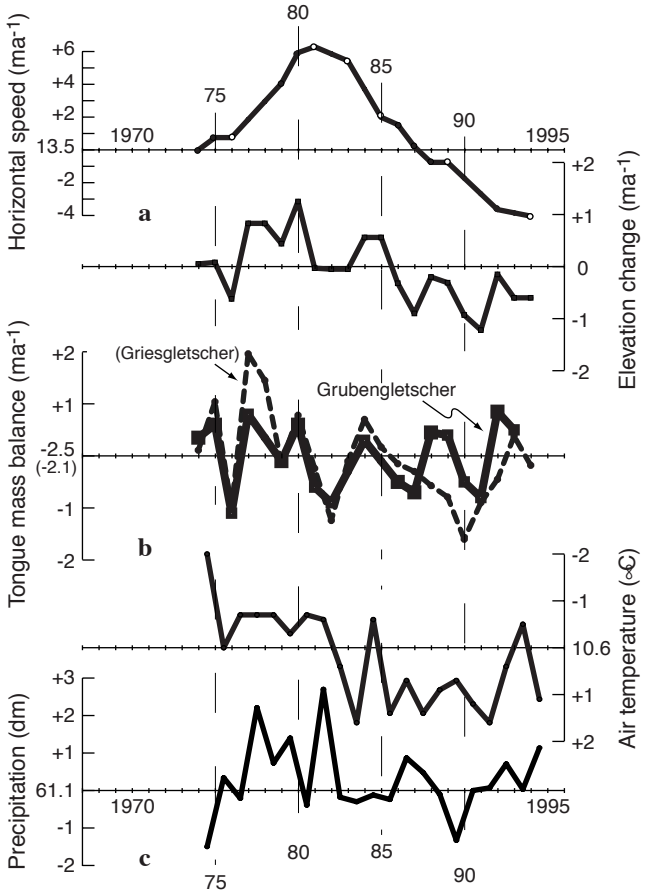

Figure 11